RSC Advances

PAPER

View Article Online
View Journal | View Issue

Check for updates

Cite this: *RSC Adv.*, 2023, **13**, 16584

Magnetic polyborate nanoparticles as a green and efficient catalyst for one-pot four-component synthesis of highly substituted imidazole derivatives†

Alireza Malihishoja,[a] Mohammad G. Dekamin *[a] and Mohammad Eslami[b]

Received 5th April 2023
Accepted 6th May 2023

DOI: 10.1039/d3ra02262e

rsc.li/rsc-advances

In this study, magnetic polyborate nanoparticles (MPBNPs) were prepared *via* a simple procedure from boric acid by using ball-milling and then characterized by various spectroscopic, microscopic and analytical methods including FT-IR, EDX, XRD, FESEM, VSM and TGA analysis. The obtained MPBNPs were further explored, as a green and highly efficient catalyst, in the multi-component synthesis of a wide range of tetra-substituted imidazoles from cascade cyclocondensation as well as *in situ* air oxidation of benzil or benzoin, aromatic aldehydes, primary amine and ammonium acetate in EtOH, as a green solvent, under reflux conditions. Additionally, environmentally friendly conditions for the preparation of the catalyst by the use of non-toxic reactants, facile procedure and high to excellent yields of the desired products as well as the use of a green solvent are some advantages of this new protocol.

1. Introduction

Nowadays, the development of simple, inexpensive, less hazardous and more efficient protocols for the synthesis of organic compounds in higher yields and atom efficiency as well as with shorter reaction times is one of the important goals of green chemistry. Following this goal, many catalytic systems have been investigated to facilitate the progress of organic reactions and be used in both fine and bulk chemicals production.[1–11]

Among all of these, magnetic nanoparticles (MNPs) have attracted lots of attention by providing promising properties as supports for different catalytic systems due to their appropriate surface area and magnetic properties. The magnetic feature of such catalysts facilitates their separation from the mixture after its completion. These magnetic catalysts have been utilized in Brønsted acid/or base, transitional metal, organo- and enzymatic catalysis reactions. Hence, being specifically robust, chemically stable as well as readily available with a naturally low toxicity and cost has made them efficient alternatives to other well-known catalyst supports especially silica and alumina.[12–57] As the case of our study, imidazole derivatives are one of the important nitrogen-containing five-membered heterocyclic compounds. This is due to their essential role as an important scaffold in diverse active pharmaceutical ingredients (APIs) and biologically active molecules such as histidine, histamine, biotin, losartan, olmesartan, eprosartan, miconazole, ketoconazole, clotrimazole and trifenagrel (Fig. 1). Furthermore, they have been proved as efficient anti-cancer and anti-inflammation as well as anti-tuberculosis, antimicrobial and anti-anaphylaxis

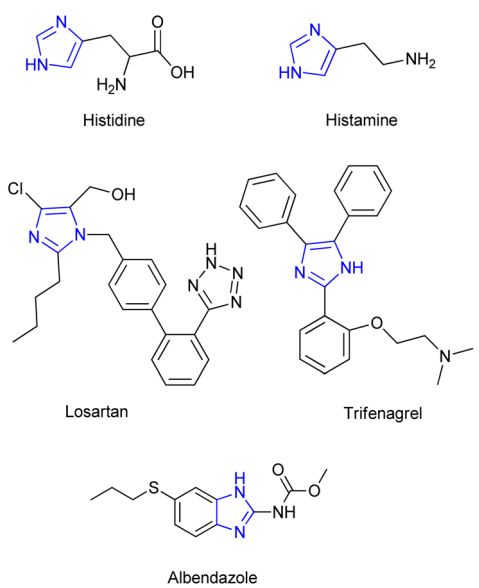

Fig. 1 Structures of some biological molecules and active pharmaceutical ingredients (APIs) containing imidazole scaffold.

[a]Pharmaceutical and Heterocyclic Compounds Research Laboratory, Department of Chemistry, Iran University of Science and Technology, Tehran 16846-13114, Iran. E-mail: mdekamin@iust.ac.ir

[b]Department of Chemistry, Behbahan Khatam Alanbia University of Technology, Behbahan 63616-63973, Iran

† Electronic supplementary information (ESI) available. See DOI: https://doi.org/10.1039/d3ra02262e

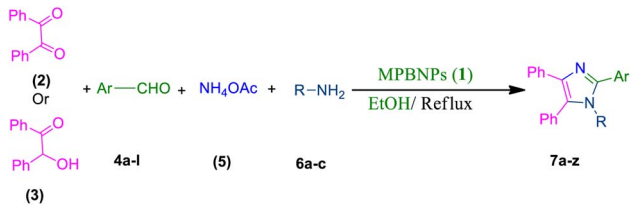

Scheme 1 One-pot four-component synthesis of tetra-substituted imidazoles **7a–z** catalyzed by the magnetic polyborate nanoparticles (MPBNPs, **1**).

compounds.[58–66] Moreover, highly-substituted 1,3-dialkylimidazoles have demonstrated their high potential in the form of ionic liquids, as green solvents, or precursors of N-heterocyclic carbenes (NHCs) as efficient organocatalysts or ligands in coordination chemistry in the recent decades.[67–71] Indeed, the potency and vast application of imidazole derivatives can be attributed to their hydrogen bond donor–acceptor capability as well as high affinity for metals, such as the zinc, iron and magnesium present in many receptor active sites of the biological systems along with anti-corrosion property. Hence, diverse applications of compounds containing imidazole as a moiety highlights the necessity of achieving efficient protocols for the synthesis of corresponding highly substituted derivatives. Following this issue, multi-component reaction (MCR) of benzyl or benzoin with aldehydes, primary amines and ammonium acetate is one of the most convenient protocols for synthesis of multi-substituted imidazole derivatives.[72–75]

Different homogeneous or heterogeneous catalytic systems have been deployed for the multi-component synthesis of substituted imidazoles including ZSM-11 or HY zeolite, dimethylpyridinium trinitromethanide, 3-picolinic acid, silica sulfuric acid, ZrO_2–Al_2O_3, ZrO_2–β-cyclodextrin, nano-Al-MCM-41, triethylammonium acetate as an ionic liquid, I_2, Keggin-type hetero polyacids, chitosan-coated Fe_3O_4 nanoparticles, Fe_3O_4–PEG–Cu, Boehmite nanoparticles, silica chloride, 2,6-pyromellitic diamide–diacid bridged mesoporous organosilica nanospheres, $(N_2H_5)_2SiF_6$ and Fe_3O_4/SiO_2 decorated trimesic acid-melamine.[6,40,76–82] Despite of their merits, there are also some disadvantages associated with these and similar procedures. These disadvantages include the use of hazardous or expensive reagents, low stability or recyclability of the catalysts as well as yields of desired products, pollution generated during the catalyst preparation, long reaction times and difficult work-up steps. Therefore, development of the productive, green and inexpensive approaches for the synthesis of multi-substituted imidazoles would be very desirable.[83]

In this work, we have presented magnetic polyborate nanoparticles (MPBNPs), as an environmental-friendly, inexpensive and efficient catalyst, in the one-pot four-component synthesis of 1,2,4,5-tetrasubstituted imidazoles in EtOH, as a green solvent, under reflux conditions (Scheme 1). Key features of this procedure are high to excellent yields of products,

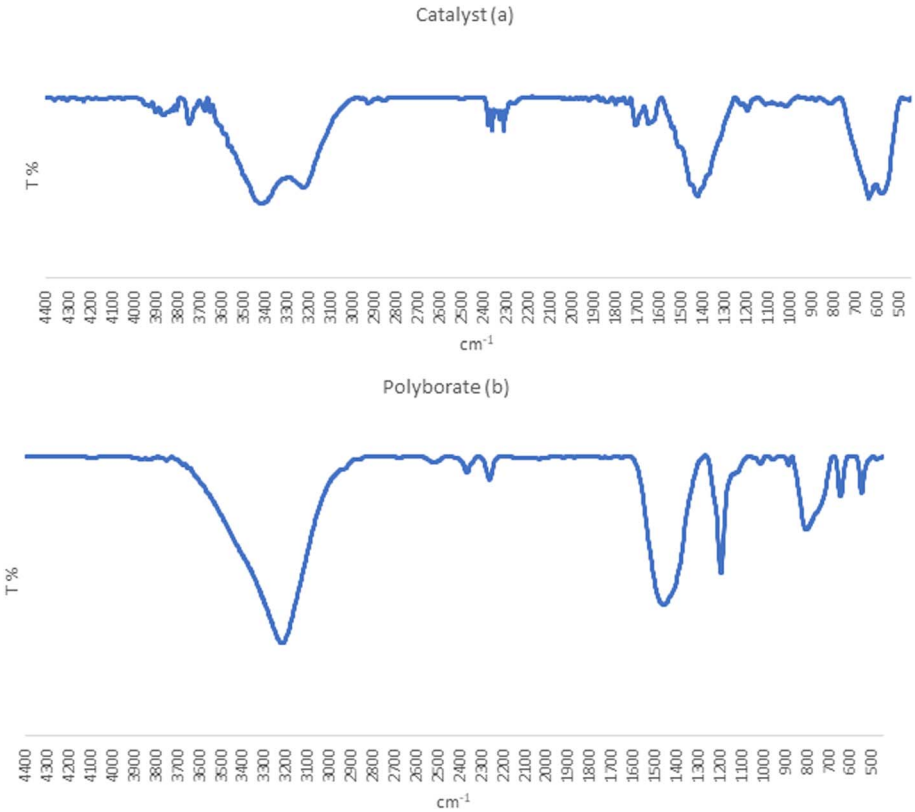

Fig. 2 Fourier transform infrared spectra of (a) MPBNPs (**1**) and (b) polyborate.

environmentally benign conditions, short reaction time and easy work-up that have made this method unique compared to others. Moreover, the catalyst is reusable at least after five runs with negligible loss in its function.

2. Experimental

2.1. General information

All chemicals were purchased from Merck and Fluka companies and used as received, except benzaldehyde (**4d**), thiophene-2-carbaldehyde (**4h**), furfural (**4k**) and aniline (**6b**), which fresh distilled samples were used. The ball mill was a Retsch MM 400 swing mill. 10 ml stainless steel ball mill vessels and two stainless steel balls with 12 mm diameter were used, and the milling frequency was set at 20 Hz at the ambient temperature. Melting points were recorded by using an Electrothermal IA 9000 apparatus. Purity of the chemicals and completion of the reactions was monitored by thin-layer chromatography (TLC) using ethyl acetate and *n*-hexane as eluting solvents. ^{1}H NMR spectra of products were measured with VARIAN – INOVA 500 MHz in DMSO or $CDCl_3$ as solvent. All products are known and characterized by measuring of their melting points (Tables 2and 3) as well as obtaining of their FT-IR and ^{1}H NMR spectra and comparison with the literature data.

2.2. Preparation method of polyborate

10.0 g of boric acid was heated at 200 °C while stirring for 5 h to form polyborate. Then, the obtained polyborate was converted into nanoscale by using ball milling for 20 min, and the milling frequency was set at 20 Hz. The structure of the obtained polyborate nanoparticles was confirmed by using FT-IR technique.

2.3. Preparation method of magnetic polyborate (MPBNPs, 1)

MPBNPs were prepared from co-precipitation of ferrous and ferric salts with polyborate nanoparticles. First, $FeCl_3 \cdot 6H_2O$ (4.0 mmol, 1.08 g) and $FeCl_2 \cdot 4H_2O$ (2.0 mmol, 0.40 g) were dissolved in 100 ml of distilled water. Then, pH of the obtained

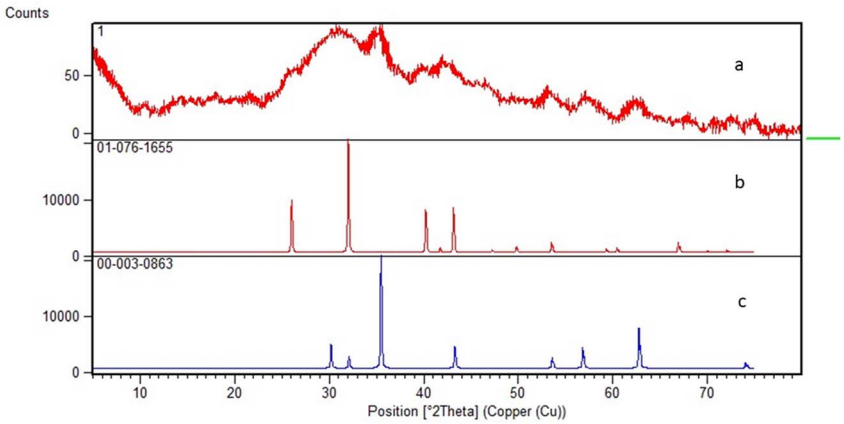

Fig. 3 XRD pattern of (a) MPBNPs catalyst (**1**); (b) Fe_3O_4 and (c) B_2O_3.

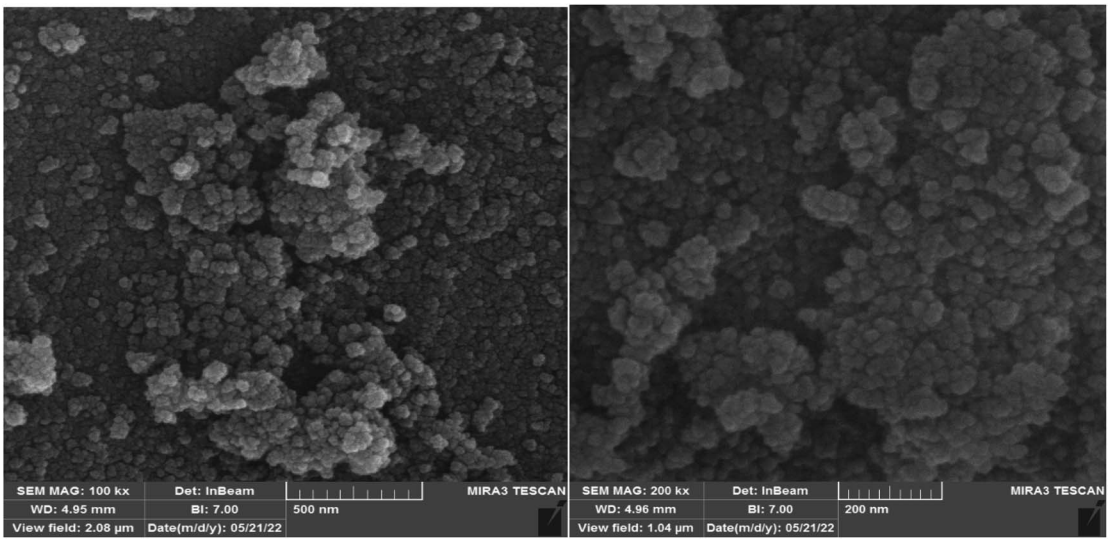

Fig. 4 FESEM images of the MPBNPs catalyst (**1**).

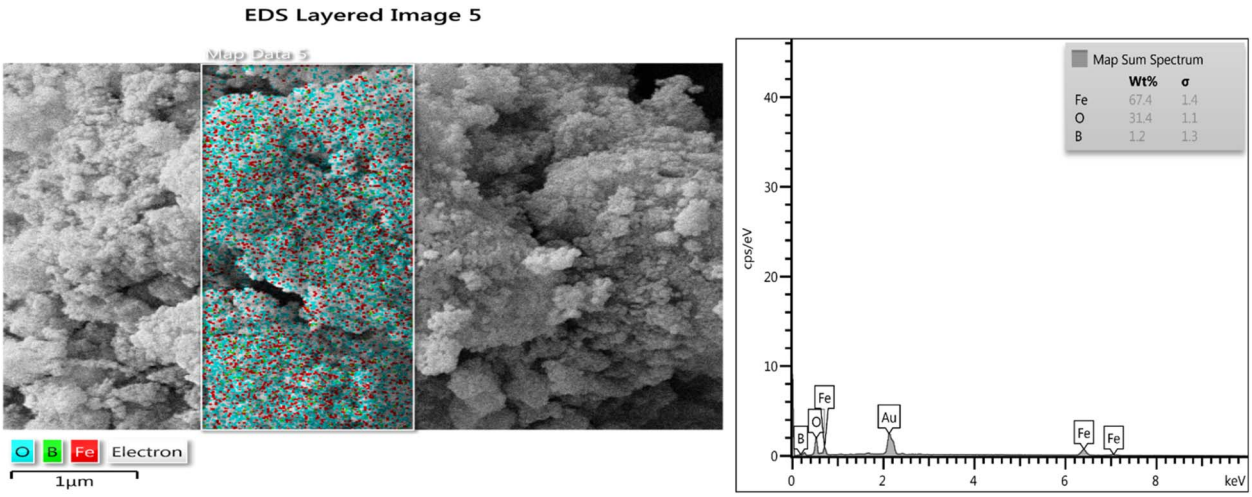

Fig. 5 EDX and mapping analysis of sample nanoparticles (**1**).

mixture was adjusted into 4.0 from 1.5 by addition of NaOH (1.0 M). Next, another mixture containing 100 mg of polyborate dispersed in 20 ml deionized water under ultrasonic was poured into the obtained mixture by vigorous stirring. After 30 min mixing, pH of the mixture was adjusted into 10.0 using NaOH (1.0 M). Afterward, the obtained mixture was stirred for 1 h and the nanoparticles of magnetic polyborate were washed with double distilled water (2.0 ml) three times and finally separated by using an external magnet and put into an oven at 50 °C to dry for 5 h.

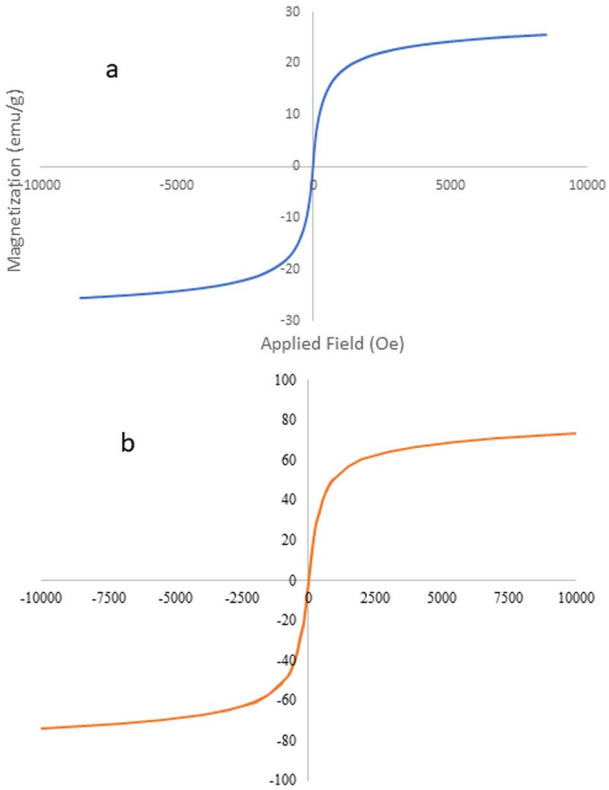

Fig. 6 VSM pattern of the magnetic polyborate nanoparticles (a) *vs.* the Fe_3O_4 reference (b).[56]

2.4. General procedure for the synthesis of 1,2,4,5-tetrasubstituted imidazoles 7a–z catalyzed by the MPBNPs (1)

10.0 mg of the MPBNPs catalyst (**1**) was added to a round-bottom flask containing benzyl or benzoin (**2** or **3**, 1.0 mmol), aldehyde (**4a–l**, 1.0 mmol), primary amine (**6a**, 1.0 mmol) and ammonium acetate (**5**, 1.75 mmol) in EtOH (2.5 ml) and the obtained mixture was heated under reflux conditions. After completion of the reaction monitored by TLC, additional EtOH (2–3 ml) was used to dissolve the products and remain the insoluble MPBNPs (**1**). The obtained mixture was heated and filtered off to separate the magnetic catalyst **1** using an external magnet. Distilled water was added dropwise to the filtrate at 50 °C to afford pure crystals of the desired products **7a–p**. The separated magnetic catalyst **1** was suspended in EtOH (2 ml) and filtered off three times and then dried in an oven at 50 °C for 5 h before using in the next runs.

2.5. Spectral data of the selected derivatives of imidazoles (7e, 7h, 7k, 7l, 7m, 7w, 7r)

2.5.1. 1-Benzyl-2-(4-methoxyphenyl)-4,5-diphenyl-1*H*-imidazole (7e). Mp: 144–147 °C; white solid; FTIR (KBr; cm^{-1}): 3026, 2929, 2361, 1605, 1530, 1482, 1449; ^{1}H NMR (500 MHz, $CDCl_3$, ppm): δ 7.62–7.56 (m, 3H), 7.42–7.10 (m, 12H), 6.92 (d, J = 8.0 Hz, 2H), 6.82 (dd, J = 7.7, 1.7 Hz, 2H), 5.09 (s, 2H), 3.88–3.76 (m, 3H).

2.5.2. 1-Benzyl-4,5-diphenyl-2-(thiophen-2-yl)-1*H*-imidazole (7h). Mp: 160–161 °C; yellow solid; FTIR (KBr; cm^{-1}): 3427, 3050, 2376, 1598, 1496, 1444; ^{1}H NMR (500 MHz, DMSO-d_6, ppm): δ 7.61 (dt, J = 7.0, 1.5 Hz, 1H), 7.50–7.39 (m, 6H), 7.34–7.12 (m, 8H), 7.06 (m, 1H), 6.92 (d, J = 7.6 Hz, 2H), 5.26 (s, 2H).

2.5.3. 2-(3-Nitrophenyl)-1,4,5-triphenyl-1*H*-imidazole (7k). Mp: 258–259 °C; yellow solid; FTIR (KBr; cm^{-1}): 3427, 1525, 1344, 766, 697; ^{1}H NMR (500 MHz, DMSO-d_6, ppm): δ 8.96 (s,

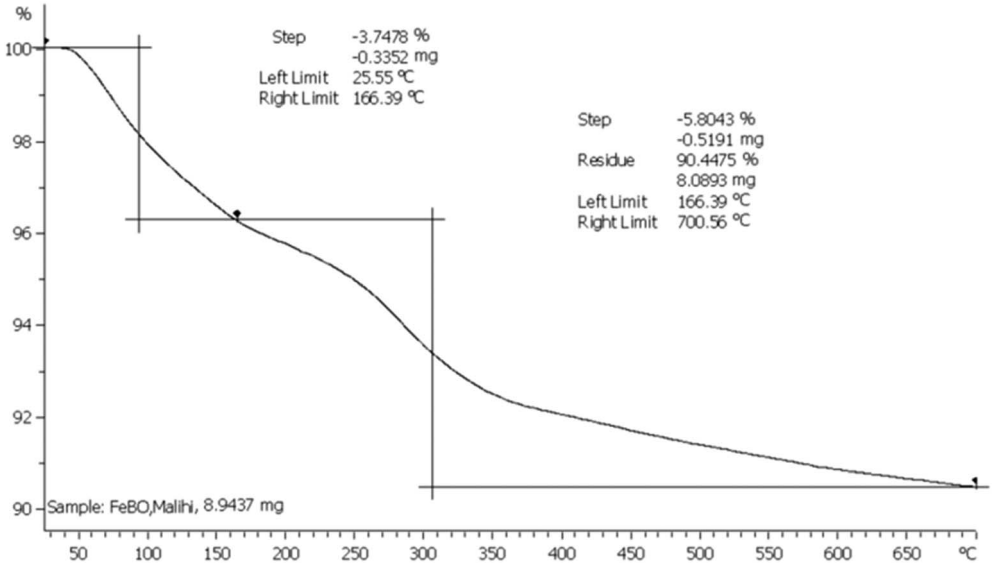

Fig. 7 TGA curve of the MPBNPs catalyst (**1**).

1H), 8.52 (d, J = 8.0 Hz, 1H), 8.22 (d, J = 8.0 Hz, 1H), 8.18–8.10 (m, 1H), 7.78 (td, J = 8.2, 1.7 Hz, 1H), 7.62–7.19 (m, 14H).

2.5.4. 1,2,4,5-Tetraphenyl-1*H*-imidazole (7l). Mp: 219–221 °C; white solid; FTIR (KBr; cm^{-1}): 3048, 2360, 1596, 1498, 770, 692; ^{1}H NMR (500 MHz, $CDCl_3$, ppm): δ 7.62 (s, 5H), 7.45 (s, 5H), 7.14 (s, 5H), 7.05 (s, 5H).

2.5.5. *N*,*N*-Dimethyl-4-(1,4,5-triphenyl-1*H*-imidazol-2-yl) aniline (7m). Mp: 206–2027 °C; brown solid; FTIR (KBr; cm^{-1}): 3422, 2926, 2364, 1722, 1612, 1488, 1442, 1370, 816, 694; ^{1}H NMR (500 MHz, DMSO-d_6, ppm): δ 7.60–7.50 (m, 1H), 7.47 (d, J = 7.5 Hz, 1H), 7.35–7.30 (m, 6H), 7.21 (m, 10H), 6.57 (d, J = 8.5 Hz, 2H), 2.88 (s, 6H).

Table 1 Systematic study for optimization of four-component reaction between benzil (**2**), 4-chlorobenzaldehyde (**4a**), ammonium acetate (**5**) and benzylamine (**6a**) under different conditions[a]a

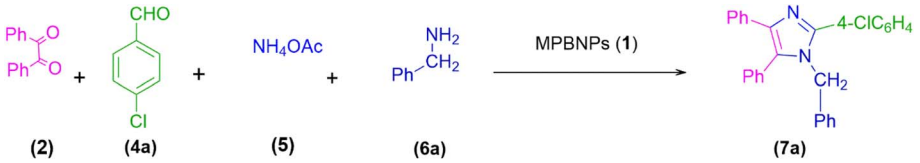

Entry	Catalyst loading (mg)	Solvent	Temp. (°C)	Time (min)	Yield[b] (%)
1	—	EtOH	r.t	240	Trace
2	MPBNPs (**1**, 5.0 mg)	MeOH	r.t	60	35
3	MPBNPs (**1**, 5.0 mg)	H_2O	r.t	60	28
4	MPBNPs (**1**, 5.0 mg)	EtOH	r.t	60	45
5	MPBNPs (**1**, 5.0 mg)	EtOAc	r.t	60	21
6	MPBNPs (**1**, 5.0 mg)	CH_3CN	r.t	60	30
7	MPBNPs (**1**, 5.0 mg)	THF	r.t	60	Trace
8	MPBNPs (**1**, 5.0 mg)	H_2O/MeOH	r.t	60	46
9	MPBNPs (**1**, 5.0 mg)	H_2O/EtOH	r.t	60	53
10	MPBNPs (**1**, 2.5 mg)	ETOH	Reflux	40	25
11	MPBNPs (**1**, 5.0 mg)	ETOH	Reflux	40	69
12	MPBNPs (**1**, 7.5 mg)	ETOH	Reflux	40	88
13	**MPBNPs (1, 10.0 mg)**	**ETOH**	**Reflux**	**40**	**96**
14	PB (10.0 mg)	ETOH	Reflux	40	66
15	Fe_3O_4 (10.0 mg)	ETOH	Reflux	40	44
16[c]	MPBNPs (10.0 mg)	ETOH	Ultrasound	40	67
17[d]	MPBNPs (10.0 mg)	ETOH	Microwave	40	85

[a] Reaction conditions: benzil (**2**, 1.0 mmol), 4-chlorobenzaldehyde (**4a**, 1.0 mmol), ammonium acetate (**5**, 1.75 mmol), benzylamine (**6a**, 1.0 mmol) and magnetic polyborate catalyst (**1**) at different conditions. [b] Isolated yield. [c] The use of ultrasound as energy source. [d] The use of microwave as energy source.

Table 2 Synthesis of 1,2,4,5-tetrasubstituted imidazoles *via* one-pot four-component condensation of benzil (**2**), aromatic aldehydes **4a–l**, ammonium acetate (**5**) and primary amines (**6a–c**) in the presence of MPBNPs catalyst (**1**)[a]

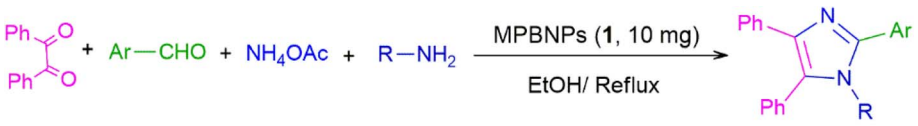

(**2**) (**4a-l**) (**5**) (**6a-c**) (**7a-z**)

Entry	ArCHO (**4**)	R–NH$_2$ (**6**)	Product (**7**)	Time (min)	Yield (%)	Mp (°C)	Mp (°C) [ref.]
1	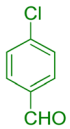 **4a**	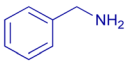 **6a**	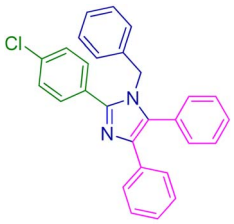 **7a**	40	96	161–162	162–160 (ref. 6)
2	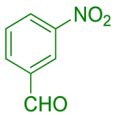 **4b**	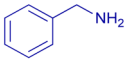 **6a**	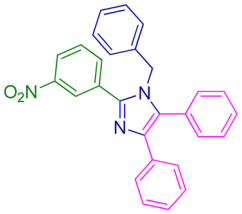 **7b**	42	92	150–151	152–154 (ref. 70)
3	 **4c**	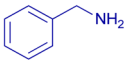 **6a**	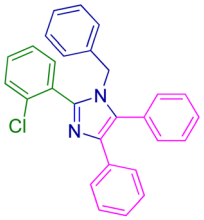 **7c**	50	86	142–143	141–142 (ref. 45)
4	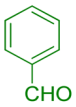 **4d**	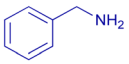 **6a**	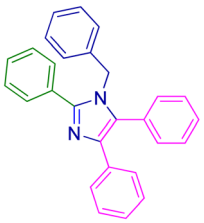 **7d**	58	90	159–161	161–163 (ref. 11)
5	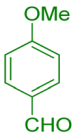 **4e**	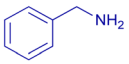 **6a**	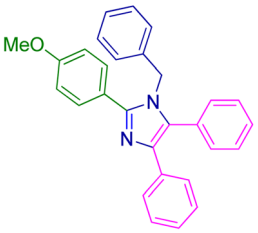 **7e**	60	88	155–156	155–157 (ref. 11)

Table 2 (*Contd.*)

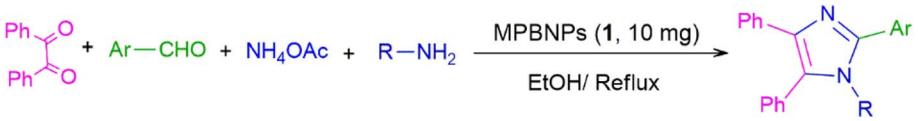

(2) (4a-l) (5) (6a-c) (7a-z)

Entry	ArCHO (4)	R–NH$_2$ (6)	Product (7)	Time (min)	Yield (%)	Mp (°C)	Mp (°C) [ref.]
6	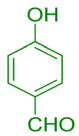 4f	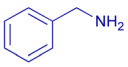 6a	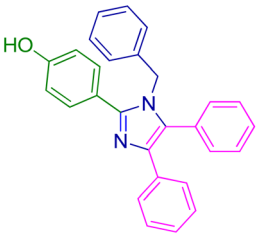 7f	59	92	132–133	131–132 (ref. 11)
7	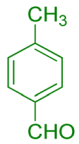 4g	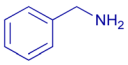 6a	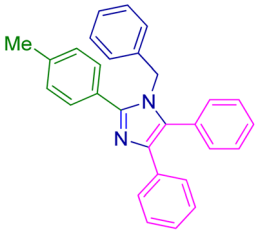 7g	55	90	164–165	167–168 (ref. 8)
8	 4h	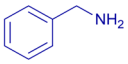 6a	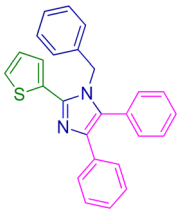 7h	60	85	178–179	177–179 (ref. 63)
9	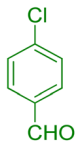 4a	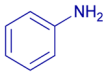 6b	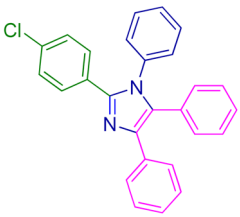 7i	44	94	168–169	167–168 (ref. 45)
10	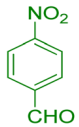 4i	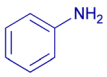 6b	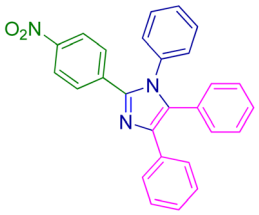 7j	46	90	210–212	212–214 (ref. 6)

Table 2 (*Contd.*)

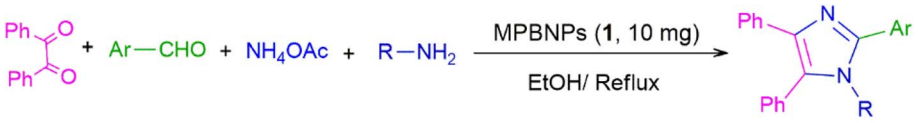

(2) (4a-l) (5) (6a-c) (7a-z)

Entry	ArCHO (4)	R–NH$_2$ (6)	Product (7)	Time (min)	Yield (%)	Mp (°C)	Mp (°C) [ref.]
11	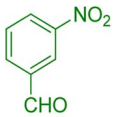 4b	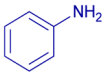 6b	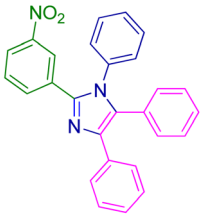 7k	50	86	250–251	250–252 (ref. 70)
12	 4d	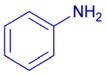 6b	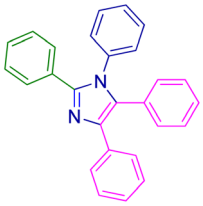 7l	50	88	219–220	220–221 (ref. 45)
13	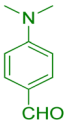 4j	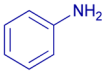 6b	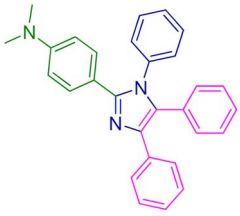 7m	55	89	206–208	207–209 (ref. 20)
14	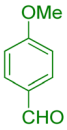 4e	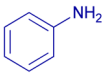 6b	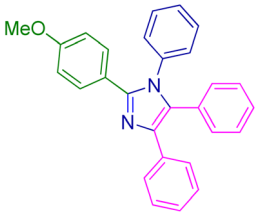 7n	59	83	181–183	182–184 (ref. 53)
15	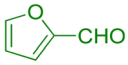 4k	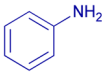 6b	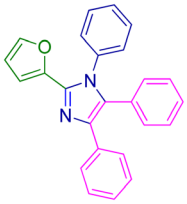 7o	60	80	203–205	200–209 (ref. 45)

Table 2 (*Contd.*)

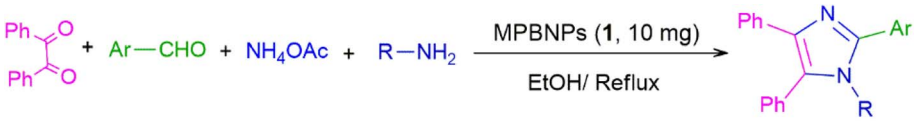

(2) (4a-l) (5) (6a-c) (7a-z)

Entry	ArCHO (4)	R–NH_2 (6)	Product (7)	Time (min)	Yield (%)	Mp (°C)	Mp (°C) [ref.]
16	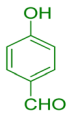 4f	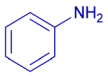 6b	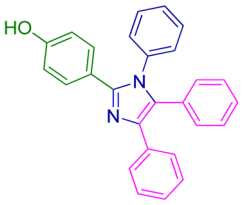 7p	60	86	282–284	281–284 (ref. 45)
17	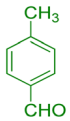 4g	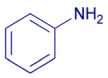 6b	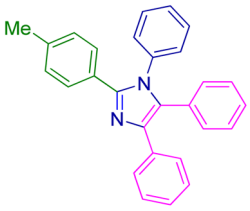 7q	57	84	200–201	200–203 (ref. 45)
18	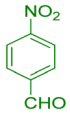 4i	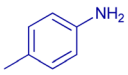 6c	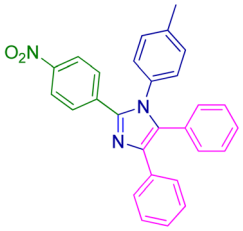 7r	46	90	219–221	218–220 (ref. 44)
19	 4l	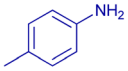 6c	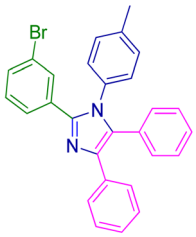 7s	50	89	156–158	158–160 (ref. 70)
20	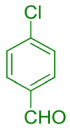 4a	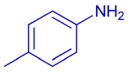 6c	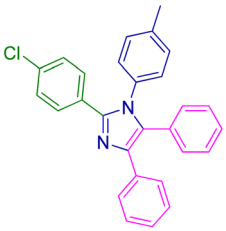 7t	42	95	164–165	166–168 (ref. 63)

Table 2 (*Contd.*)

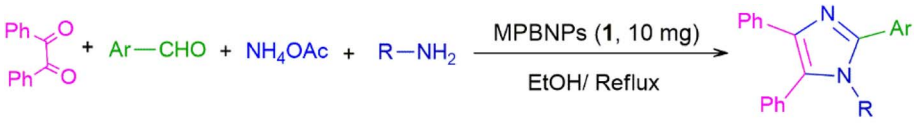

(2) (4a-l) (5) (6a-c) (7a-z)

Entry	ArCHO (4)	R–NH_2 (6)	Product (7)	Time (min)	Yield (%)	Mp (°C)	Mp (°C) [ref.]
21	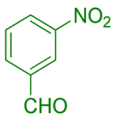 4b	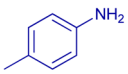 6c	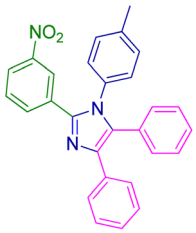 7u	48	92	146–148	146–149 (ref. 45)
22	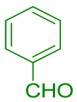 4d	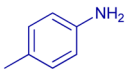 6c	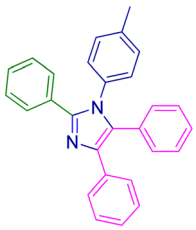 7v	60	90	173–174	172–174 (ref. 44)
23	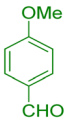 4e	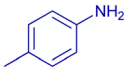 6c	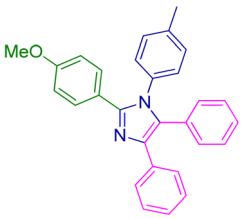 7w	68	84	179–180	180–181 (ref. 18)
24	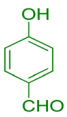 4f	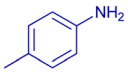 6c	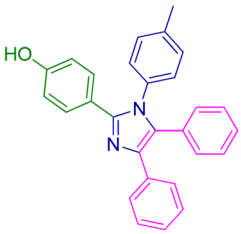 7x	70	89	297–299	298–300 (ref. 63)
25	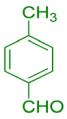 4g	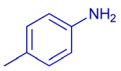 6c	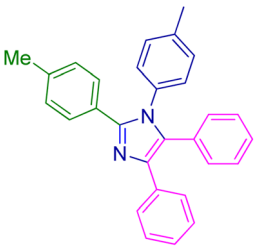 7y	62	85	189–191	189–191 (ref. 63)

Table 2 (*Contd.*)

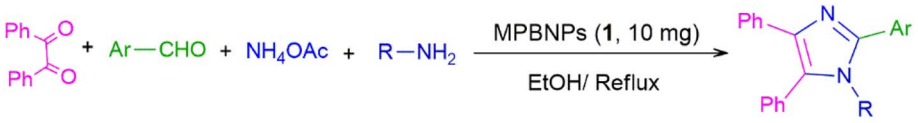

(2) (4a-l) (5) (6a-c) (7a-z)

Entry	ArCHO (4)	R–NH$_2$ (6)	Product (7)	Time (min)	Yield (%)	Mp (°C)	Mp (°C) [ref.]
26	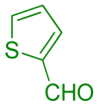 4h	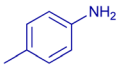 6c	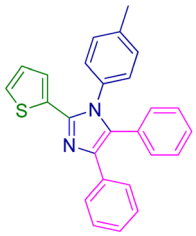 7z	60	82	200–201	200–203 (ref. 45)

[a] Reaction conditions: benzil (**2**, 1.00 mmol), aromatic aldehyde (**4a–l**, 1.00 mmol), ammonium acetate (**5**, 1.75 mmol), primary amine (**6a–c**, 1.00 mmol) and catalyst (**1**, 10.0 mg) in EtOH (2.5 ml) under reflux conditions.

2.5.6. 2-(4-Nitrophenyl)-4,5-diphenyl-1-(*p*-tolyl)-1*H*-imidazole (7r). Mp: 218–219 °C; yellow solid; FTIR (KBr; cm^{-1}): 3032, 2922, 2852, 2366, 1532, 1352, 750, 694; ^{1}H NMR (500 MHz, DMSO-d_6, ppm): δ 7.98 (s, 1H), 7.73–7.56 (m, 3H), 7.50–7.39 (m, 2H), 7.33 (dt, J = 6.0, 3.5 Hz, 3H), 7.27–7.21 (m, 4H), 7.20–7.14 (m, 1H), 7.03 (t, J = 10.5 Hz, 4H), 2.18 (s, 3H).

2.5.7. 2-(4-Methoxyphenyl)-4,5-diphenyl-1-(*p*-tolyl)-1*H*-imidazole (7w). Mp: 179–180 °C; white solid; FTIR (KBr; cm^{-1}): 2922, 2376, 1606, 1514, 1438, 1368, 1022, 824, 776, 698, 526; ^{1}H NMR (500 MHz, DMSO-d_6, ppm): δ 7.49–7.44 (m, 2H), 7.34–7.26 (m, 5H), 7.26–7.19 (m, 4H), 7.19–7.06 (m, 5H), 6.88–6.82 (m, 2H), 3.73 (s, 3H), 2.26 (s, 3H).

3. Results and discussion

3.1. Characterization of the magnetic polyborate nanoparticles (1)

Prepared MPBNPs were characterized by different spectroscopic, microscopic and analytical methods and techniques such as Fourier transform infrared spectroscopy (FT-IR), X-ray powder diffraction (XRD), field emission scanning electron microscopy (FESEM), energy-dispersive X-ray (EDX) spectroscopy, vibrating sample magnetometer (VSM) and thermogravimetric analysis (TGA).

3.1.1. Fourier transform infrared (FT-IR) analysis. As shown in Fig. 2, Fourier transform infrared spectroscopy for primary identification of the MPBNPs catalyst (**1**) was employed. The band appeared at 638 cm^{-1} is related to stretching vibrations of the Fe–O bonds of Fe_3O_4 magnetic nanoparticles.[80] Also, the absorption bands at 1232 and 1430 cm^{-1} can be attributed to the symmetric and asymmetric stretching vibrations of B–OH and B–O bonds of polyborate nanoparticles, respectively.[84] On the other hand, the absorption band in the range of 3208–3410 cm^{-1} corresponds to the stretching vibrations of the acidic OH groups in structure of MPBNPs, which is a broad band due to strong intermolecular hydrogen bonding between OH groups. In general, according to these observed data it can be suggested that the MPBNPs (**1**) have been prepared successfully.

3.1.2. X-Ray powder diffraction analysis. The XRD pattern was obtained with copper target (λ = 1.54 Å) at the range of 10–80° for 2θ. Main diffraction peaks at 2θ = 27.06, 32.64, 33.83, 35.43, 36.36, 42.84, 45.38, 50.10, 57.80° are adapted with the reference patterns of corresponding structure of MPBNPs (Fig. 3). Also, the crystallographic structure of Fe_3O_4 did not change during the process for preparation of the catalyst **1**. Moreover, the size of nanoparticles was calculated to be about 35.28 nm based on the Debye–Scherrer equation according to peak of 2θ = 32.64°.

3.1.3. Field emission scanning electron microscopy (FESEM) analysis. FESEM analysis was performed to investigate the size and morphology of the catalyst **1**. The recorded images proved the nano dimension of particles besides spherical nature of them in the structure of catalyst (Fig. 4). Also, according to the FESESM micrograms the average size of nanoparticles is estimated to be about 36 nm that demonstrates good consistency with the XRD results.

3.1.4. Energy dispersive X-ray (EDX) and mapping analysis. The presence of anticipated elements such as boron, oxygen and iron was justified by EDX technique. Furthermore, uniform distribution of boron atoms in the structure of the catalyst is clear in the elemental mapping analysis (Fig. 5).

3.1.5. Vibrating sample magnetometer (VSM). The magnetic property of MPBNPs (**1**) was examined by vibrating sample magnetometer. It was measured out at room temperature under magnetic field −8500 to +8500 oersted. According to

Table 3 Synthesis of 1,2,4,5-tetrasubstituted imidazoles *via* one-pot four-component condensation of benzoin (**3**), aromatic aldehydes **4**, ammonium acetate (**5**) and primary amines (**6a–c**) in the presence ofMPBNPs catalyst (**1**)[a]

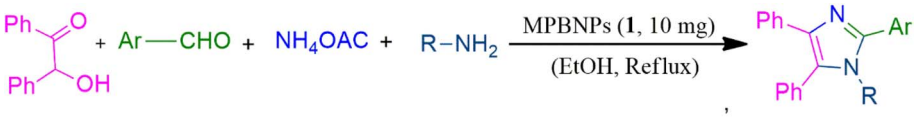

(**3**) (**4**) (**5**) (**6a-c**) (**7**)

Entry	ArCHO (**4**)	R–NH$_2$ (**6**)	Product (**7**)	Time (min)	Yield[b] (%)	Mp (°C)	Mp (°C) [ref.]
1	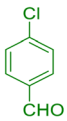 **4a**	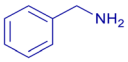 **6a**	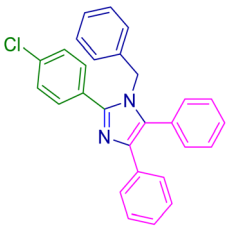 **7a**	42	96	161–162	162–164 (ref. 6)
2	 **4d**	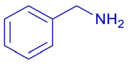 **6a**	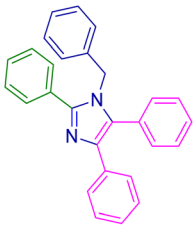 **7d**	52	90	160–161	161–163 (ref. 11)
3	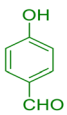 **4f**	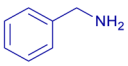 **6a**	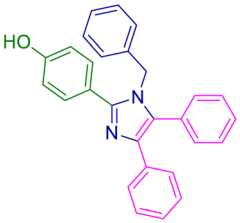 **7f**	60	85	132–133	131–132 (ref. 11)
4	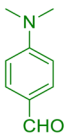 **4j**	 **6b**	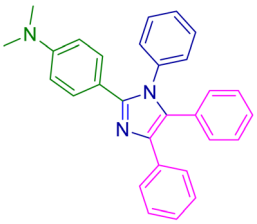 **7m**	58	89	207–208	207–209 (ref. 20)
5	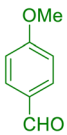 **4e**	 **6b**	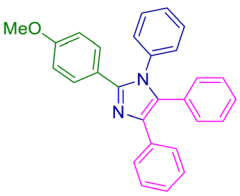 **7n**	55	93	181–183	182–184 (ref. 70)

Table 3 (*Contd.*)

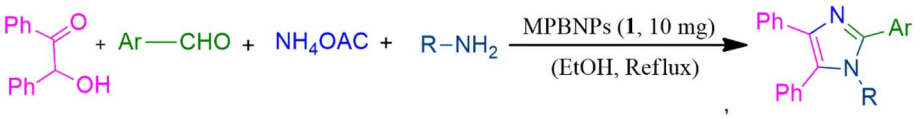

(3) (4) (5) (6a-c) (7)

Entry	ArCHO (4)	R–NH_2 (6)	Product (7)	Time (min)	Yield[b] (%)	Mp (°C)	Mp (°C) [ref.]
6	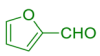 4k	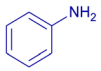 6b	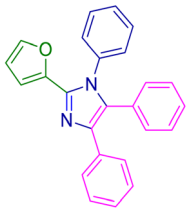 7o	54	82	201–202	200–209 (ref. 44)
7	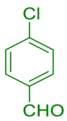 4a	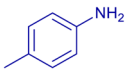 6c	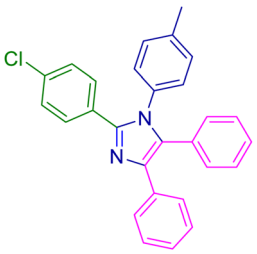 7t	46	92	164–165	166–168 (ref. 45)
8	 4l	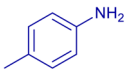 6c	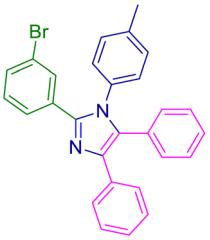 7s	50	85	156–158	158–160 (ref. 70)
9	 4d	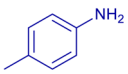 6c	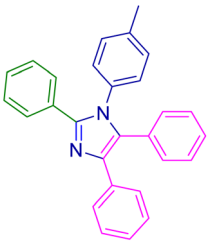 7v	54	90	171–173	172–174 (ref. 44)
10	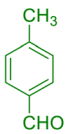 4g	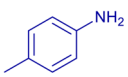 6c	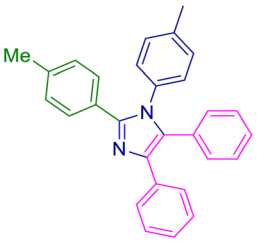 7y	60	87	187–189	189–191 (ref. 63)

Table 3 (*Contd.*)

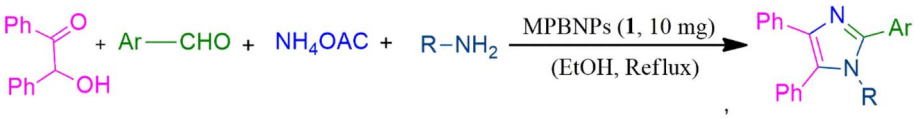

(3) (4) (5) (6a-c) (7)

Entry	ArCHO (4)	R–NH_2 (6)	Product (7)	Time (min)	Yield[b] (%)	Mp (°C)	Mp (°C) [ref.]
11	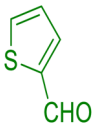 4h	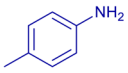 6c	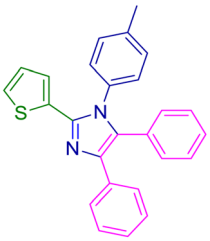 7z	57	82	198–200	200–203 (ref. 45)

[a] Reaction conditions: benzoin (**3**, 1.00 mmol), aromatic aldehyde (**4**, 1.00 mmol), ammonium acetate (**5**, 1.75 mmol), primary amine (**6a–c**, 1.00 mmol) and catalyst (**1**, 10.0 mg) in EtOH (2.5 ml) under reflux conditions. [b] Isolated yield.

values obtained from VSM analysis, the magnetization saturation for MPBNPs is 24.03715 emu g^{-1}. The S-shaped curve shown in Fig. 6 proves the magnetic behavior of the MPBNPs catalyst (**1**).[85]

3.1.6. Thermogravimetric analysis (TGA). The thermal stability of the MPBNPs nanoparticles (**1**) was investigated by TGA-DTG analysis at the range of 25–700 °C. As shown in Fig. 7, thermogram illustrate two steps for weight losses. The first step is between 25 to 166 °C, which was associated with physically or chemically adsorbed water in the structure of the catalyst with 3.75% loss in the initial weight of sample. The second step of weight loss occurred between 166 and 700 °C, which counted 5.80% of the total weight and can be attributed to condensation of OH groups on the surface of MPBNPs (**1**).

3.2. Optimization of conditions in synthesis of tetra-substituted imidazoles

To show the efficiency of the MPBNPs catalyst (**1**) for the synthesis of the 1,2,4,5-tetrasubstituted imidazoles, the reaction of benzil (**2**, 1.00 mmol), 4-chlorobenzaldehyde (**4a**, 1.00 mmol), ammonium acetate (**5**, 1.75 mmol) and benzylamine (**6a**, 1.00 mmol) was carried out as a model reaction (Table 1). The reaction conditions were optimized into the best catalyst loading, solvent and energy input for the synthesis of 1-benzyl-2-(4-chlorophenyl)-4,5-diphenyl-1*H*-imidazole (**7a**). The results are shown in Table 1. Indeed, the yeild of the desired product **7a** in the absence of catalyst **1** even after 4 h in the EtOH at room temperature was trace (entry 1). Moreover, the effect of the catalyst loading to proceed the model reaction was investigated in the next experiments (entries 10–13). Whereas loading of 5.0 mg of the MPBNPs catalyst (**1**) increased the yield of desired product **7a** in EtOH at room temperature after 60 min to about 45%, the reaction yield increased to about 69% under reflux conditions with same amount of the catalyst **1** loading. Also, the reaction was examined in other solvents such as H_2O, MeOH, EtOAc, CH_3CN and THF under the same conditions and all of them afforded lower yields than EtOH (entries 2–9). Polarity of EtOH and solubility of the components of reaction in EtOH beside formation of hydrogen bonds with the produced water from cycloaddition are some rational reasons for getting higher yields by using EtOH as a solvent. On the other hand, when the model reaction was carried out in EtOH under reflux conditions by loading 5.0 mg of the catalyst **1** afforded higher yield of desired product **7a**. Furthermore, the amount of the obtained product **7a** under the same condition was increased significantly after loading 10.0 mg of the MPBNPs catalyst (**1**) to 96% (entry 13). Additionally, completion of the model reaction in the presence of PB and Fe_3O_4 individually was examined (entries 14 and 15) and synergic effect between them justifies promising results. Finally, the effect of ultrasound and microwave radiation on the reaction rate was investigated (entries 16 and 17). Consequently, 10.0 mg MPBNPs (**1**) loading in EtOH under reflux conditions was chosen as the optimized conditions in the next experiments (Tables 2 and 3).

3.3. The proposed mechanism for the synthesis of tetra-substituted imidazole derivatives in the presence of MPBNPs catalyst (1)

The most probable mechanism for the formation of tetra-substituted imidazoles has been represented in Scheme 2. In fact, the electrophilicity of the carbonyl groups of aldehydes **4** is increased by involving in the interaction with the Lewis acidic

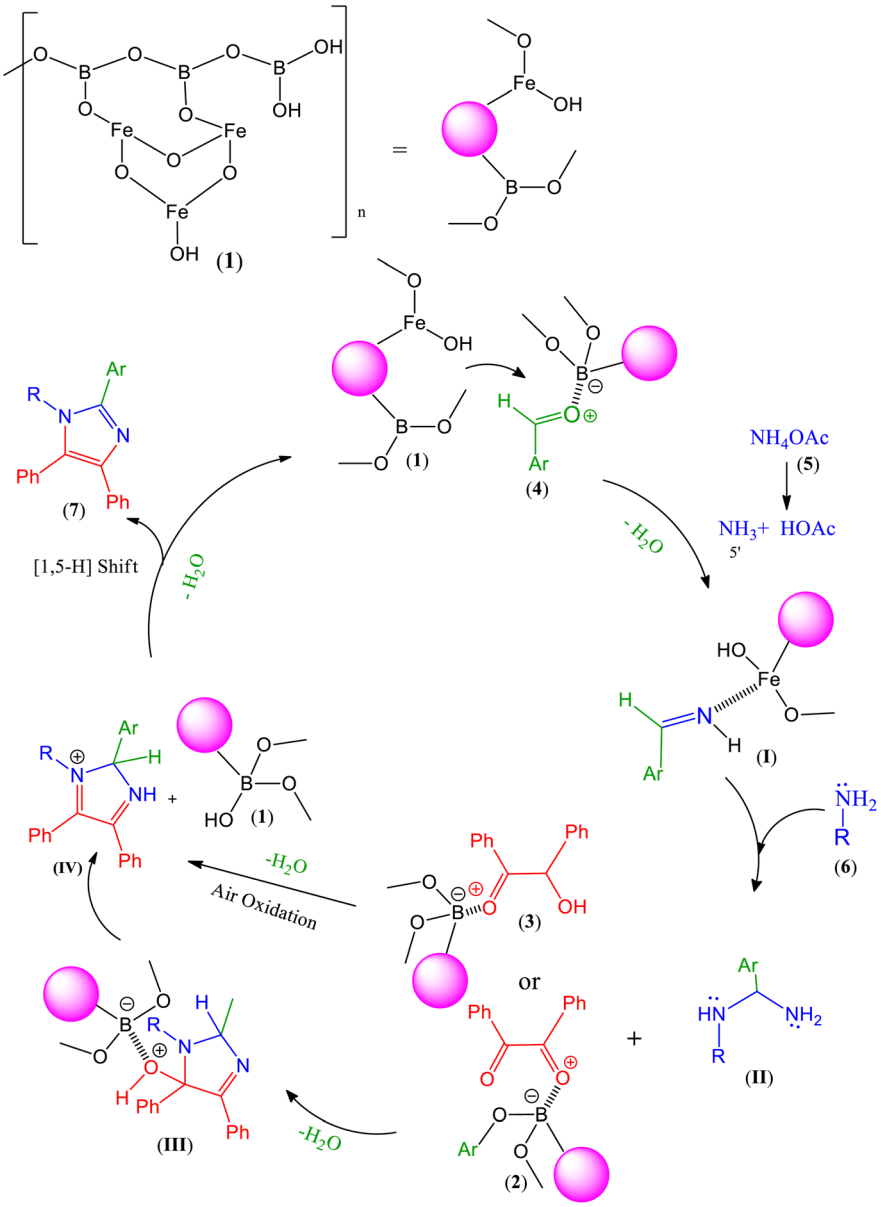

Scheme 2 Feasible mechanism for the synthesis of 1,2,4,5-tetra-substituted imidazoles **7** in the presence of MPBNPs (**1**).

centers of both B and Fe atoms of the MPBNPs catalyst (**1**). Then, nucleophiles including ammonia (**5′**) and amines **6** can be added to the activated carbonyl group of aldehydes **4** to afford the corresponding imine (**I**) and aminal (**II**) intermediates, respectively. After that, the obtained intermediate **II** reacts with the activated benzil (**2**) or benzoin (**3**) carbonyl groups to produce cyclic intermediate **III** and **IV**, respectivly. The later intermediate is formed by losing one molecules of water through simple imine condensation and subsequent air oxidation in the case of benzoin. Desired imidazole derivatives **7** are finally produced after a [1,5-H] shift and the liberated MPBNPs (**1**) can start a new cycle of its catalytic activity.[40,77,82]

The reusability of the MPBNPs catalyst (**1**) was also investigated for the model reaction in another part of our study. After completion of the reaction, the catalyst **1** was separated

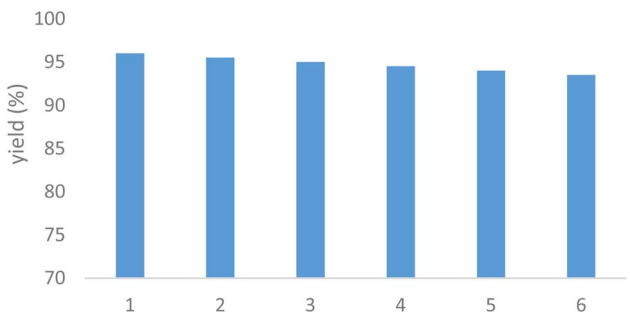

Fig. 8 Reusability of the heterogeneous MPBNPs catalyst (**1**) in the model reaction to afford **7a**.

Table 4 Comparative data for the activity of different catalysts for the synthesis of 7a

Entry	Catalyst	Catalyst loading	Reaction conditions	Time (min)	Yield (%)
1	3-Picolinic acid[6]	12 mg	EtOH/80 °C	120	96
2	PANI–$FeCl_3$ (ref. 86)	200 mg	CH_3CN/reflux	1440	83
3	PMAMOSa[40]	15 mg	EtOH/reflux	45	95
4	Nano-$TiCl_4 \cdot SiO_2$ (ref. 87)	100 mg	Solvent-free/130 °C	30	95
5	$K_5CoW_{12}O_{40} \cdot 3H_2O$[88]	32	Solvent-free/140 °C	180	90
6	Magnetic polyborate nanoparticles	10 mg	EtOH/reflux	40	96 (This work)
7	Sulfonic acid functionalized silica[89]	20 mg	Solvent-free/140 °C	100	94

using an external magnet and suspended in EtOH. Afterward, it was filtered off three times and then dried in an oven at 50 °C for 5 h before using in the next runs. The obtained results are summarized in Fig. 8. As it can be observed, the catalyst **1** is reusable for at least five runs with negligible loss in its activity.

To demonstrate the catalytic efficiency of the MPBNPs catalyst (**1**) for the synthesis of 1,2,4,5-tetrasubstituted imidazoles, its performance has been compared with some acidic catalytic systems in the model reaction. The results are summarized in Table 4. The provided data clearly illustrate that the MPBNPs catalyst (**1**) is superior to many introduced catalytic systems for the synthesis of 1,2,4,5-tetrasubstituted imidazole derivatives in terms of the catalyst loading, shorter reaction time, the use of a green solvent, working at lower temperature and reusability of the catalyst for more runs with keeping its activity.

4. Conclusions

In summary, an efficient, environmentally benign, non-hazardous and expeditious protocol for the synthesis of highly-substituted imidazoles has been described in this work. Simple preparation of the magnetic polyborate nanoparticles (MPBNPs) catalyst by using ball-milling technique and its easy separation from the reaction mixture by an external magnetic field as well as accessibility of the reagents are key features of this new protocol and its superiorities to other catalytic systems. The new MPBNPs were applied in the condensation of benzil (or benzoin), aromatic carbocyclic and heterocyclic aldehydes, ammonium acetate and primary amines to afford the corresponnding highly-substituted imidazoles, which are greatly important in numerous of biological and pharmacological compounds. Moreover, it was found that the use of EtOH, as a green solvent, affords the highest yields of the desired products.

Conflicts of interest

There are no conflicts to declare.

Acknowledgements

We are grateful for the financial support from The Research Council of Iran University of Science and Technology (IUST), Tehran, Iran (Grant No.: 160/22061) is highly appreciated. The partial financial support of The Iran Nanotechnology Initiative Council (INIC) is gratefully acknowledged. Mohammad Eslami is also very thankful for the support of the Iran National Science Foundation (INSF).

References

1 R. V. Orru and E. Ruijter, *Synthesis of heterocycles via multicomponent reactions II*, Springer Science & Business Media, 2010.
2 J. Zhu and H. Bienaymé, *Multicomponent reactions*, John Wiley & Sons, 2006.
3 D. J. Ramón and M. Yus, *Angew. Chem., Int. Ed.*, 2005, **44**, 1602–1634.
4 A. Keivanloo, M. Bakherad, E. Imanifar and M. Mirzaee, *Appl. Catal., A*, 2013, **467**, 291–300.
5 A. Khazaei, A. R. Moosavi-Zare, F. Gholami and V. Khakyzadeh, *Appl. Organomet. Chem.*, 2016, **30**, 691–694.
6 A. Z. Al Munsur, H. N. Roy and M. K. Imon, *Arabian J. Chem.*, 2020, **13**, 8807–8814.
7 J. J. Gabla, S. R. Mistry and K. C. Maheria, *Catal. Sci. Technol.*, 2017, **7**, 5154–5167.
8 K. C. Nicolaou, T. Montagnon and S. A. Snyder, *Chem. Commun.*, 2003, 551–564, DOI: 10.1039/b209440c.
9 B. H. Rotstein, S. Zaretsky, V. Rai and A. K. Yudin, *Chem. Rev.*, 2014, **114**, 8323–8359.
10 C. de Graaff, E. Ruijter and R. V. Orru, *Chem. Soc. Rev.*, 2012, **41**, 3969–4009.
11 M. G. Dekamin, M. Azimoshan and L. Ramezani, *Green Chem.*, 2013, **15**, 811–820.
12 B. Jiang, T. Rajale, W. Wever, S. J. Tu and G. Li, *Chem.–Asian J.*, 2010, **5**, 2318–2335.
13 X. B. Wang, L. He, T. Y. Jian and S. Ye, *Chin. Chem. Lett.*, 2012, **23**, 13–16.
14 M. A. Silver and T. E. Albrecht-Schmitt, *Coord. Chem. Rev.*, 2016, **323**, 36–51.
15 L. Lv, Y. Chen, A. Shatskiy, J. Q. Liu, X. Liu, M. D. Kärkäs and X. S. Wang, *Eur. J. Org. Chem.*, 2021, **2021**, 964–968.
16 S. Balalaie and A. Arabanian, *Green Chem.*, 2000, **2**, 274–276.
17 R. C. Cioc, E. Ruijter and R. V. Orru, *Green Chem.*, 2014, **16**, 2958–2975.
18 M. G. Dekamin, Z. Karimi, Z. Latifidoost, S. Ilkhanizadeh, H. Daemi, M. R. Naimi-Jamal and M. Barikani, *Int. J. Biol. Macromol.*, 2018, **108**, 1273–1280.
19 D. M. Perrine, J. T. Ross, S. J. Nervi and R. H. Zimmerman, *J. Chem. Educ.*, 2000, **77**, 1479.

20 B. Dai, Y. Duan, X. Liu, L. Song, M. Zhang, W. Cao, S. Zhu, H. Deng and M. Shao, *J. Fluorine Chem.*, 2012, **133**, 127–133.
21 M. Rahman, A. K. Bagdi, D. Kundu, A. Majee and A. Hajra, *J. Heterocycl. Chem.*, 2012, **49**, 1224–1228.
22 Z. Tavakoli, M. Baghernegh ad and K. Niknam, *J. Heterocycl. Chem.*, 2012, **49**, 634–639.
23 Y. Wan, G. x. Liu, L. l. Zhao, H. y. Wang, S. y. Huang, L. f. Chen and H. Wu, *J. Heterocycl. Chem.*, 2014, **51**, 713–718.
24 S. A. Laufer, W. Zimmermann and K. J. Ruff, *J. Med. Chem.*, 2004, **47**, 6311–6325.
25 M. M. Heravi, F. Derikvand and F. F. Bamoharram, *J. Mol. Catal. A: Chem.*, 2007, **263**, 112–114.
26 M. M. Heravi, E. Hashemi, Y. S. Beheshtiha, K. Kamjou, M. Toolabi and N. Hosseintash, *J. Mol. Catal. A: Chem.*, 2014, **392**, 173–180.
27 M. Kidwai, P. Mothsra, V. Bansal, R. K. Somvanshi, A. S. Ethayathulla, S. Dey and T. P. Singh, *J. Mol. Catal. A: Chem.*, 2007, **265**, 177–182.
28 A. Shaabani and A. Rahmati, *J. Mol. Catal. A: Chem.*, 2006, **249**, 246–248.
29 A. Teimouri and A. N. Chermahini, *J. Mol. Catal. A: Chem.*, 2011, **346**, 39–45.
30 H. R. Shaterian and M. Ranjbar, *J. Mol. Liq.*, 2011, **160**, 40–49.
31 L. Wu, X. Jing, H. Zhu, Y. Liu and C. Yan, *J. Chil. Chem. Soc.*, 2012, **57**, 1204–1207.
32 M. M. Khodaei, K. Bahrami and I. Kavianinia, *J. Chin. Chem. Soc.*, 2007, **54**, 829–833.
33 B. Sadeghi, B. Mirjalili, S. Bidaki and M. Ghasemkhani, *J. Iran. Chem. Soc.*, 2011, **8**, 648–652.
34 L. F. Tietze and A. Modi, *Med. Res. Rev.*, 2000, **20**, 304–322.
35 K. Bahrami, M. M. Khodaei and A. Nejati, *Monatsh. Chem.*, 2011, **142**, 159–162.
36 B. Das, J. Kashanna, R. A. Kumar and P. Jangili, *Monatsh. Chem.*, 2013, **144**, 223–226.
37 M. M. Heravi, F. Derikvand and M. Haghighi, *Monatsh. Chem.*, 2008, **139**, 31–33.
38 M. S. Patil, C. K. Khatri and G. U. Chaturbhuj, *Monatsh. Chem.*, 2018, **149**, 1453–1457.
39 C. Wu, A. Alqahtani, S. Sangtarash, A. Vezzoli, H. Sadeghi, C. M. Robertson, C. Cai, C. J. Lambert, S. J. Higgins and R. J. Nichols, *Nanoscale*, 2020, **12**, 7914–7920.
40 E. Valiey and M. G. Dekamin, *Nanoscale Adv.*, 2022, **4**, 294–308.
41 S. Karami, M. G. Dekamin, E. Valiey and P. Shakib, *New J. Chem.*, 2020, **44**, 13952–13961.
42 Z. Zarnegar and J. Safari, *New J. Chem.*, 2014, **38**, 4555–4565.
43 D. A. Shabalin and J. E. Camp, *Org. Biomol. Chem.*, 2020, **18**, 3950–3964.
44 Y. Zhu, C. Li, J. Zhang, M. She, W. Sun, K. Wan, Y. Wang, B. Yin, P. Liu and J. Li, *Org. Lett.*, 2015, **17**, 3872–3875.
45 R. B. Sparks and A. P. Combs, *Org. Lett.*, 2004, **6**, 2473–2475.
46 S. E. Wolkenberg, D. D. Wisnoski, W. H. Leister, Y. Wang, Z. Zhao and C. W. Lindsley, *Org. Lett.*, 2004, **6**, 1453–1456.
47 B. Maleki, G. E. Kahoo and R. Tayebee, *Org. Prep. Proced. Int.*, 2015, **47**, 461–472.
48 F. Zhang, Q. Gao, B. Chen, Y. Bai, W. Sun, D. Lv and M. Ge, *Phosphorus, Sulfur Silicon Relat. Elem.*, 2016, **191**, 786–789.
49 L. F. Tietze and N. Rackelmann, *Pure Appl. Chem.*, 2004, **76**, 1967–1983.
50 M. Esmaeilpour, J. Javidi, F. Dehghani and S. Zahmatkesh, *Res. Chem. Intermed.*, 2017, **43**, 163–185.
51 H. FaniMoghadam, M. G. Dekamin and N. Rostami, *Res. Chem. Intermed.*, 2022, **48**, 3061–3089.
52 H. Hanoon, E. Kowsari, M. Abdouss, M. Ghasemi and H. Zandi, *Res. Chem. Intermed.*, 2017, **43**, 4023–4041.
53 S. J. Saghanezhad, M. H. Sayahi, I. Imanifar, M. Mombeni and S. Deris Hamood, *Res. Chem. Intermed.*, 2017, **43**, 6521–6536.
54 M. G. Dekamin, E. Arefi and A. Yaghoubi, *RSC Adv.*, 2016, **6**, 86982–86988.
55 M. G. Dekamin, S. Ilkhanizadeh, Z. Latifidoost, H. Daemi, Z. Karimi and M. Barikani, *RSC Adv.*, 2014, **4**, 56658–56664.
56 T. T. Nguyen, N.-P. T. Le and P. H. Tran, *RSC Adv.*, 2019, **9**, 38148–38153.
57 N. Rostami, M. G. Dekamin, E. Valiey and H. FaniMoghadam, *RSC Adv.*, 2022, **12**, 21742–21759.
58 M. Salimi, M. A. Nasseri, T. D. Chapesshloo and B. Zakerinasab, *RSC Adv.*, 2015, **5**, 33974–33980.
59 N. Thimmaraju and S. M. Shamshuddin, *RSC Adv.*, 2016, **6**, 60231–60243.
60 E. Valiey and M. G. Dekamin, *RSC Adv.*, 2022, **12**, 437–450.
61 Z. Zarnegar and J. Safari, *RSC Adv.*, 2014, **4**, 20932–20939.
62 A. Akbari, M. G. Dekamin, A. Yaghoubi and M. R. Naimi-Jamal, *Sci. Rep.*, 2020, **10**, 10646.
63 N. Rostami, M. G. Dekamin, E. Valiey and H. Fanimoghadam, *Sci. Rep.*, 2022, **12**, 8642.
64 S. Safapoor, M. G. Dekamin, A. Akbari and M. R. Naimi-Jamal, *Sci. Rep.*, 2022, **12**, 10723.
65 M. Sam, M. G. Dekamin and Z. Alirezvani, *Sci. Rep.*, 2021, **11**, 2399.
66 S. Rostamnia and E. Doustkhah, *Synlett*, 2015, **26**, 1345–1347.
67 T. D. A. Kumar, N. Yamini, C. Subrahmanyam and K. Satyanarayana, *Synth. Commun.*, 2014, **44**, 2256–2268.
68 A. Davoodnia, M. M. Heravi, Z. Safavi-Rad and N. Tavakoli-Hoseini, *Synth. Commun.*, 2010, **40**, 2588–2597.
69 M. G. Dekamin, M. Eslami and A. Maleki, *Tetrahedron*, 2013, **69**, 1074–1085.
70 A. Padwa and S. K. Bur, *Tetrahedron*, 2007, **63**, 5341.
71 S. Samai, G. C. Nandi, P. Singh and M. Singh, *Tetrahedron*, 2009, **65**, 10155–10161.
72 C. Mukhopadhyay, P. K. Tapaswi and M. G. Drew, *Tetrahedron Lett.*, 2010, **51**, 3944–3950.
73 K. Niknam, A. Deris, F. Naeimi and F. Majleci, *Tetrahedron Lett.*, 2011, **52**, 4642–4645.
74 M. S. Patil, A. V. Palav, C. K. Khatri and G. U. Chaturbhuj, *Tetrahedron Lett.*, 2017, **58**, 2859–2864.
75 D. S. Rekunge, C. K. Khatri and G. U. Chaturbhuj, *Tetrahedron Lett.*, 2017, **58**, 4304–4307.
76 R. Rossi, G. Gaetano, G. Casotti, C. Manzini and M. Lessi, *Adv. Synth. Catal.*, 2019, **361**, 2737–2803.
77 M. A. Zolfigol, S. Baghery, A. R. Moosavi-Zare and S. M. Vahdat, *RSC Adv.*, 2015, **5**, 32933–32940.

78 S. S. Dipake, V. D. Ingale, S. A. Korde, M. K. Lande, A. S. Rajbhoj and S. T. Gaikwad, *RSC Adv.*, 2022, **12**, 4358–4369.
79 B. Sadeghi, B. B. F. Mirjalili and M. M. Hashemi, *Tetrahedron Lett.*, 2008, **49**, 2575–2577.
80 K. Sivakumar, A. Kathirvel and A. Lalitha, *Tetrahedron Lett.*, 2010, **51**, 3018–3021.
81 F. El hajri, Z. Benzekri, H. Anahmadi, S. Sibous, A. Ouasri, A. Souizi, A. Hassikou, A. Rhandour and S. Boukhris, *Inorg. Chim. Acta*, 2022, **536**, 120915.
82 B. Fattahi and M. G. Dekamin, *Sci. Rep.*, 2023, **13**, 401.
83 I. V. Machado, J. R. Dos Santos, M. A. Januario and A. G. Corrêa, *Ultrason. Sonochem.*, 2021, **78**, 105704.
84 P. Qi, S. Wang, W. Wang, J. Sun, H. Yuan and S. Zhang, *Int. J. Biol. Macromol.*, 2022, **205**, 261–273.
85 Z. Alirezvani, M. G. Dekamin and E. Valiey, *Sci. Rep.*, 2019, **9**, 17758.
86 M. Abdollahi-Alibeik and M. Moosavifard, *Synth. Commun.*, 2010, **40**, 2686–2695.
87 B. F. Mirjalili, A. H. Bamoniri and L. Zamani, *Sci. Iran.*, 2012, **19**, 565–568.
88 L. Nagarapu, S. Apuri and S. Kantevari, *J. Mol. Catal. A: Chem.*, 2007, **266**, 104–108.
89 G. Mohammadi Ziarani, Z. Dashtianeh, M. Shakiba Nahad and A. Badiei, *Arabian J. Chem.*, 2015, **8**, 692–697.